International Journal of Adhesion & Adhesives 104 (2021) 102723

Contents lists available at ScienceDirect

International Journal of Adhesion and Adhesives

journal homepage: http://www.elsevier.com/locate/ijadhadh

Examining the effect of graphene nanoplatelets on the corrosion resistance of epoxy coatings

Sotirios Kopsidas *, Ganiu B. Olowojoba, Anthony J. Kinloch, Ambrose C. Taylor

Department of Mechanical Engineering, Imperial College London, London, SW7 2AZ, UK

ARTICLE INFO

Keywords:
A
Epoxy
B
Steels
D
Durability
Coatings

ABSTRACT

Graphene due to its two-dimensional structure, large surface area and high impermeability is regarded as an excellent potential filler for the development of anti-corrosive coatings by creating a natural barrier to the diffusion of electrolytes. Epoxy polymers are widely used as protective coatings, and in the present study, commercially-available graphene nanoplatelets (GNPs) were dispersed into an epoxy resin using three-roll milling (3RM). The GNP-modified epoxy was coated onto mild steel substrates, and cured. The coated panels were immersed into a corrosive environment of 3.5 wt% NaCl aqueous solution for 4–5 days. The adhesion of the coatings to the substrate was then measured using a cross-cut test. The addition of higher loadings of GNPs resulted in a deteriorating corrosion performance, with the 1.5 wt% and 3 wt% coatings exhibiting 53% and 91% damage by area, respectively, after the cross-cut tests. The unmodified epoxy and low GNP content coatings ($\leq$0.5 wt%) demonstrated 0% damage. This shows that the corrosion behaviour of GNP/epoxy coatings is not dominated by barrier effects but by electrochemical factors. The addition of GNPs is only effective at low loadings, as higher contents result in electrically-conductive coatings that facilitate the conduction of corrosion currents.

1. Introduction

Epoxy resins are the most common class of organic protective coatings, used for the corrosion protection of metallic structures [1]. Epoxy resins have highly desirable properties in their application as coatings, due to their high strength, good chemical resistance and ease of processing [2]. In general, the anti-corrosive action of organic coatings is enhanced through the addition of functional fillers which protect against corrosion through three main mechanisms. The first type are barrier fillers which act by increasing the diffusion path of corrosive species; the second are inhibitive fillers, such as chromates and phosphates that interfere with the corrosion process; and the third are sacrificial fillers, such as zinc [1]. Zinc is a corrosion-active filler which sacrificially corrodes with respect to the metal substrate, thus providing cathodic protection [3]. Barrier fillers typically include high aspect ratio platelets, such as clays and other two-dimensional (2D) materials. Such barrier fillers can form a brick wall-type structure, where the diffusion of corrosive species through the coating is considerably delayed by being forced to follow a tortuous path, thus giving excellent barrier properties against gases and moisture [4]. Several studies have reported that the incorporation of nanoclays in polymeric matrices had a positive effect on the reduction of vapour permeability [5] and on improving the corrosion resistance of metal substrates [3,4,6].

Graphene has been considered as a highly promising material for the development of anti-corrosion barrier coatings due to its large surface area of 2630 m^2/g [7], unique 2D structure, high impermeability and inert nature to oxidation. Prasai et al. [8] reported that graphene films directly grown on copper (Cu) and nickel (Ni) substrates by chemical vapour deposition (CVD), decreased the corrosion rate by seven and by twenty times compared to the bare Cu and bare Ni, respectively.

Electrochemical techniques have been used extensively to study the effect of the addition of graphene and graphene-related materials on the anti-corrosive properties of epoxy coatings coated onto steel substrates [9–14]. However, it is not possible to predict the real-life performance of coatings in corrosive environments from electrochemical results, as the physical significance of the electrochemical results is difficult to interpret. Hence, in this study, the corrosion behaviour of epoxy coatings modified with graphene nanoplatelets (GNPs) is investigated through an exposure test where coated steel substrates are immersed in an aqueous solution of 3.5 wt% NaCl. The adhesion of the coating to the substrate is

* Corresponding author.
E-mail address: s.kopsidas15@imperial.ac.uk (S. Kopsidas).

https://doi.org/10.1016/j.ijadhadh.2020.102723

Available online 7 September 2020

measured using the cross-cut test, as a qualitative way of determining the coating's resistance to corrosion. GNPs represent one of the most common forms of commercially-available graphene; being an ultra-thin form of graphite, consisting of more than 10 graphene layers but not exceeding thicknesses of 100 nm [7]. The GNPs were dispersed into an epoxy polymer via three-roll milling (3RM) and the thermal, mechanical and electrical properties of the bulk nanocomposites were characterised. The cross-cut test results, along with results from the literature on the electrochemical behaviour of epoxy coatings modified with graphitic materials, are used to deduce the effects of the GNP fillers on the corrosion resistance of mild steel substrates coated with the various epoxy polymers.

2. Materials and manufacturing

2.1. Materials

An anhydride-cured epoxy polymer was used. The epoxy formulation comprised a 50:50 by mass mixture of a cycloaliphatic epoxy resin (Araldite CY184; Huntsman, Switzerland) with an epoxide equivalent weight (EEW) of 172 g/eq and an internally-flexibilised diglycidyl ether of bisphenol-A (DGEBA)-type epoxy (Araldite PY4122; Huntsman, Switzerland) with an EEW of 330 g/eq. Graphene nanoplatelets (GNPs) with an average lateral size of 4.5 μm, average platelet thickness of 12 nm and surface area of 80 m^2/g (Grade AO-3; Graphene Supermarket, USA) were used [15]. The value of the EEW of the blend was then calculated and the stoichiometric amount of the curing agent was added to the mixture. The curing agent was an accelerated methylhexahydrophthalic acid anhydride (Albidur HE600; Evonik, Germany) with an anhydride equivalent weight (AEW) of 170 g/eq. Ready to use, pre-cleaned mild steel panels (Stock number: R-46; Q-Lab, UK) with dimensions of 152 × 102 × 0.8 mm^3 were used as the substrates [16].

2.2. Manufacture of bulk epoxy polymers

The GNPs were dispersed into the liquid epoxy resin by stirring using a spatula followed by three-roll milling (3RM). The GNP/epoxy mixtures were passed through a three-roll mill (80E; EXAKT, Germany) eight times at a roller speed of 220 rpm and a temperature of 25 °C. For the most highly filled mixture (i.e. 3 wt%) the temperature of the rollers was set at 40 °C due to the relatively high viscosity of the mixture. The curing agent was added to the pre-dispersed resin and mixed using a mechanical stirrer (RZR 2012; Heidolph, Germany) fitted with a radial flow impeller at 500 rpm and 25 °C for 15 min. The resulting mixture was degassed in a vacuum oven at −1000 mbar for a minimum of 30 min to remove all air bubbles. For the 3 wt% mixture both mixing and degassing took place at a temperature of 40 °C. To produce bulk epoxy plates, the degassed mixtures were poured into preheated steel moulds coated with release agent (Frekote 700NC; Henkel, Germany) and then cured for 1 h at 90 °C and 2 h at 160 °C in a fan oven. The moulds were left to cool slowly to room temperature prior to the cured plates being removed.

2.3. Production of epoxy coatings

Epoxy coatings were prepared using a drawdown method, spreading the epoxy between the steel substrate and a release film, using a custom-built mould, see Fig. 1. A large and thick steel plate was used as the platen. Release agent (Frekote 700NC; Henkel, Germany) was painted onto the platen and left to dry. The steel panels were placed on top of the platen and secured using a polyester heat-resistant tape (Flashtape; Cytec, UK). A 100 μm thick polyethylene terephthalate (PET) film (Mylar A; UK Insulations, UK) was used as the release film, and was attached to the steel panel using the polyester heat-resistant tape. The mould was placed inside a cold oven, ensuring that it was level.

For the production of coatings, because the amount of resin required was minimal (approximately 5 mL for a single coating), it was convenient to prepare two concentrated GNP/epoxy masterbatches by 3RM and dilute accordingly rather than mill separate mixtures for each target concentration. A 5.21 wt% GNP/epoxy masterbatch was used for the manufacture of high GNP content coatings (i.e. 1.5 and 3 wt% loadings), while a 0.87 wt% masterbatch was used for the manufacture of low GNP content coatings (i.e. 0.125, 0.25 and 0.5 wt% loadings). The two masterbatches were diluted to the desired concentration through addition of suitable amounts of resin and curing agent. The masterbatch, resin and curing agent were poured into a 50 mL beaker and were mixed using a magnetic stir bar at 500 rpm and 25 °C for 15 min. The mixture was then degassed in a vacuum oven for 30 min at 25 °C, with the exception of the 3 wt% mixture which was stirred and degassed at 40 °C.

Following degassing, the PET film was folded back and approximately 5 mL of the GNP-modified resin was applied onto the steel panel using a plastic pipette, see Fig. 1. After the resin was applied, the PET film was allowed to fold back into place. A wire-wound drawdown bar was used to spread the resin onto the substrate. During spreading, the rod was in contact with the PET film, so the groove depth had no influence on the final coating thickness. The coating was cured in a fan oven for 1 h at 90 °C, followed by 2 h at 160 °C. The coatings were allowed to slowly cool to room temperature. The steel panel was then detached from the platen and the PET release film was carefully removed from the coating's surface.

3. Characterisation

3.1. Thermal analysis

Dynamic mechanical thermal analysis (DMTA) was performed to determine the glass transition temperature (T_g) and storage modulus (E′) of the bulk epoxy polymers using a Q800 analyser (TA Instruments, USA). Rectangular samples of 60 × 10 × 3 mm^3 were cut from the cured bulk plates and tested in dual cantilever mode. The samples were subjected to a temperature sweep from 30 °C to 200 °C at a heating rate of 2 °C/min using a frequency of 1 Hz and an oscillation strain of 0.05%.

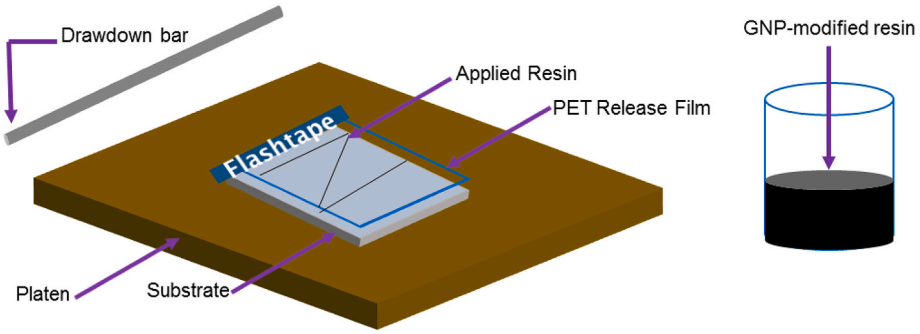

Fig. 1. Schematic of the custom-built mould used for the preparation of epoxy-coated steel panels.

The average values of T_g so determined were accurate to within about ±2 °C.

Thermogravimetric analysis (TGA) was carried out on the bulk epoxy polymers to determine their thermal stability using a TGA/DSC 1 analyser (Mettler Toledo, USA). Samples of between 5 to 15 mg were placed in a platinum crucible and were heated from 30 °C to 800 °C at a heating rate of 10 °C/min in a nitrogen atmosphere (using a flow rate of 60 mL/min).

3.2. Tensile tests

Tensile tests were conducted at room temperature using a universal testing machine (3369; Instron, UK), fitted with a 50 kN loadcell. Dumbbell specimens having a gauge length of 25 mm were machined from 75 × 13.5 × 3 mm^3 strips cut from the bulk epoxy plates. A displacement rate of 1 mm/min was used, and the strain was measured using a clip-on extensometer (2620–601; Instron, UK). The Young's modulus (E_t) was determined from the gradient of the stress versus strain curve between strains of 0.05% and 0.25% [17]. The tensile properties were averaged from the results obtained from a minimum of five specimens.

3.3. Electrical impedance spectroscopy

Electrical impedance spectroscopy (EIS) was used to measure the electrical conductivity of the bulk epoxy polymers. Samples of 10 × 10 × 2 mm^3 were coated on both surfaces with conductive silver paint and pressed between two capacitor plates in a two-electrode cell setup using a Reference 600 potentiostat (Gamry Instruments, USA). The tests were conducted inside a Faraday cage to prevent electromagnetic interference, using a root mean square alternating current (RMS AC) voltage of 10 mV over a frequency range of 100 mHz to 1 MHz. The measurements were conducted at 23 ±2 °C and 55 ±5% RH.

3.4. Exposure tests

The dry thickness of the GNP-modified epoxy coatings was measured using an electronic coating thickness gauge (456; Elcometer, UK). Twelve measurements were made across the coating's surface on non-defective sites. The coated panels were exposed to a corrosive environment of 3.5 wt% NaCl aqueous solution. The backside of the panels was protected using a primer (Hammerite red oxide; Akzo Nobel, Netherlands) and a topcoat (Bright cold galvanise; Ambersil, UK), to prevent rusting and ensure consistent water bath quality according to ASTM 870 [18]. The pH of the saline solution was measured using a HI-98107 portable pH meter (Hanna Instruments, Romania), to monitor the water quality. The fresh aqueous solution was measured to have a pH of 6.6, which is consistent with the literature [19], and throughout the exposure tests this value did not drop below a pH of 6.4. Panels were immersed to three-quarters of their height inside a filled water tank, see Fig. 2, with a maximum of four panels being accommodated. The water tank was fitted with a lid to minimise water evaporation and was placed inside an oven set at 25 °C. Immersed panels were removed from the corrosive medium at 24-h intervals to monitor the progression of corrosion. The epoxy-coated surface was rinsed with copious amounts of deionised water and then wiped dry. Images were taken with a P9 smartphone (Huawei, China) equipped with a Leica Summarit H 1:2.2/27 ASPH dual lens camera.

3.5. Cross-cut tests

The adhesion of the coating to the substrate was evaluated using a cross-cut test [20], for both exposed and unexposed panels. Prior to testing, the exposed panels were removed from the saline solution and were conditioned inside an oven set at a temperature of 23 °C for a minimum of 16 h. The cross-cut test was carried out at ambient temperature and relative humidity. Panels with a coating thickness of no greater than 60 μm, as specified by the Standard [20], were tested using a CC2000 cross hatch adhesion test kit (Dyne Testing, UK), using a knife with 6 blades each spaced 1 mm apart. Six parallel cuts were made at 0° and 90° using the multi-blade knife to form a grid. A piece of ISO2409-compliant pressure-sensitive adhesive tape was placed over the grid and rubbed firmly to ensure good contact with the coating. The tape was then pulled off steadily at an approximate angle of 60°, with the whole pull-off process not lasting longer than 1 s [20]. The area enclosed within the grid was examined with an illuminated magnifying glass to assess the degree of damage, which is taken as the area of coating detachment. The visual impression of the damage area is expressed as a percentage, which corresponds to a classification unit ranging from 0 to 5 in the Standard [20], where 0 represents no damage and 5 represents greater than 65% damage. For each panel, a minimum of three determinations was made, with the Standard stating that in the case of a greater than one classification unit mismatch, the test should be repeated at three other places, if necessary using a different panel [20].

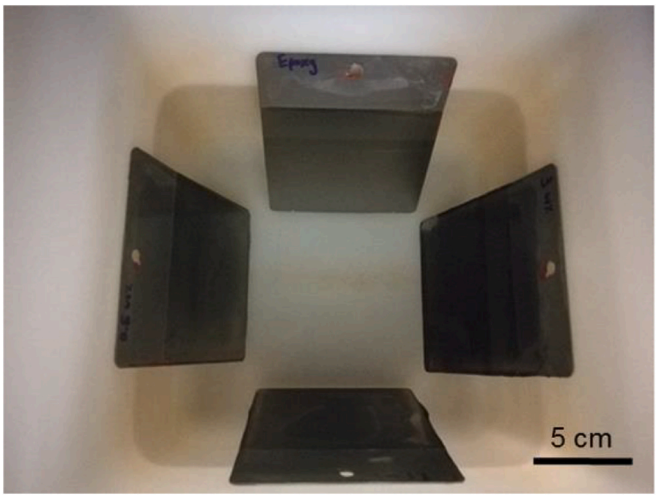

Fig. 2. Image of coating exposure tests.

For panels exposed to the corrosive environment, there was a noticeable variation in the classification of different determination points. Thus all determinations were recorded and the mean of the damage area values from each determination point was calculated. This mean damage area percentage is quoted and was used to determine the average cross-cut classification.

4. Results and discussion

4.1. Introduction

The thermal, tensile and electrical properties of the bulk unmodified epoxy and the epoxy nanocomposites modified with GNPs were determined. The steel panels coated with the GNP-modified epoxies were exposed to a saline solution of 3.5 wt% NaCl for 4–5 days. The corrosion progress was evaluated visually and the coating adhesion to the substrate was measured using the cross-cut test. The effect of the GNP nanofiller on the corrosion behaviour of the epoxy is discussed.

4.2. Bulk properties

4.2.1. Thermo-mechanical properties

The thermo-mechanical properties of the unmodified epoxy and the nanocomposites with up to 3 wt% of GNPs were determined by dynamic mechanical thermal analysis (DMTA), and are shown in Fig. 3. Values of the glass transition temperature (T_g), the glassy storage modulus ($E_g^{'}$) at 35 °C and the rubbery storage modulus ($E_r^{'}$) at 180 °C are shown in Table 1.

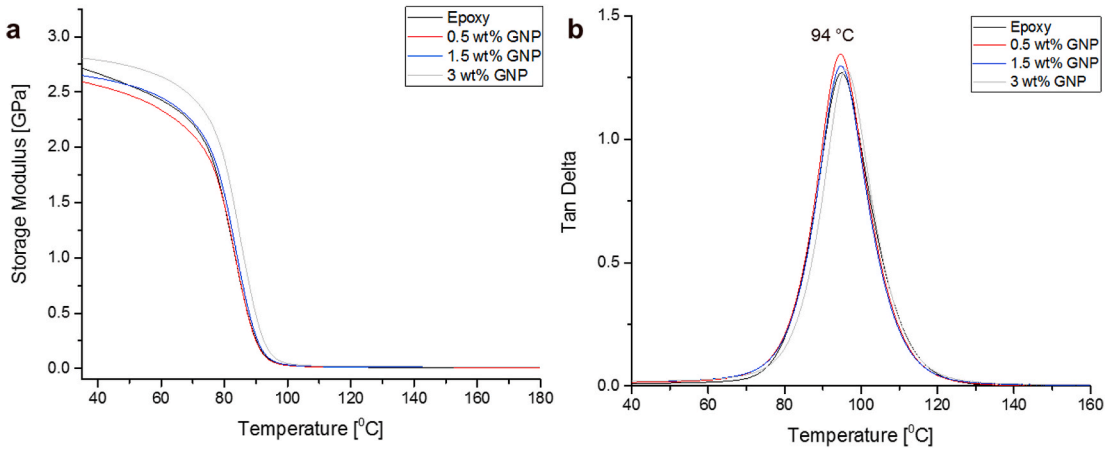

Fig. 3. Graphical representation of (a) storage modulus (E′) and (b) tan δ versus temperature for the GNP-modified epoxy nanocomposites measured using dynamic mechanical thermal analysis (DMTA).

A glassy storage modulus of 2.56 GPa was measured for the unmodified epoxy, and $E_g^{'}$ shows a marginal increase for the GNP-containing nanocomposites in comparison to the unmodified epoxy, see Table 1. The addition of the GNPs has a positive influence on the $E_r^{'}$, with a maximum increase of more than 500% to 13.6 MPa for the 3 wt %-containing nanocomposite compared to the unmodified epoxy value of 2.2 MPa, see Table 1. The $E_r^{'}$ values are related to the degree of matrix-filler interactions, with greater values indicative of a higher relaxation restriction of the macromolecular chains [21]. This is due to the presence of the stiff GNPs in the crosslinked polymer network. The incorporation of the GNPs does not have a significant effect on the T_g, as shown in Fig. 3 and Table 1. This demonstrates that the nanofiller has no effect on the final crosslinking density of the epoxy, as the GNPs do not participate in the curing reaction between the resin and curing agent due to the absence of reactive functional groups.

4.2.2. Thermal stability

The thermal stability of the unmodified epoxy and the epoxy nanocomposites in nitrogen was studied using thermogravimetric analysis (TGA). The temperature dependence of mass loss and derivative mass loss are shown in Fig. 4. The corresponding temperatures where 5% ($T_{5\%}$) and 50% ($T_{50\%}$) mass loss occurred, and where the maximum thermal degradation (T_{max}) took place, are shown in Table 2. Values of the char yield (Y_c) are also quoted, defined as the mass percentage of graphitic material remaining at the conclusion of the test at 800 °C.

The addition of the GNPs at a loading of 3 wt% has a positive influence on the thermal stability of the resulting nanocomposite. This is demonstrated by the significant increase in the onset temperature of decomposition, $T_{5\%}$, which increases by 35 °C (to 327 °C) in comparison to the unmodified epoxy, see Table 2. The incorporation of the GNPs does not influence the main degradation process, associated with the thermal oxidation of the epoxy [22], as the values of $T_{50\%}$ and T_{max} remain unchanged at about 400 °C and 405 °C, respectively. Improvements in the char yield are achieved for the GNP-containing nanocomposites; most notably the Y_c value of 11.6% obtained for the 3 wt% material, which represents an increase of 183% with respect to the unmodified epoxy. This is due to the intrinsically high heat resistance of graphene as well as its ability to promote carbonisation at the polymer/filler interface [23].

4.2.3. Tensile properties

The tensile properties of the GNP-modified epoxies are summarised in Fig. 5. The Young's modulus, E_t, increases from 2.86 ± 0.08 GPa for the unmodified epoxy to 3.28 ± 0.14 GPa for the 3 wt%-containing nanocomposite, an increase of 15%, see Fig. 5(a). For lower GNP contents (i.e. 0.5 and 1.5 wt%) there is no significant increase in E_t, which is due to the relatively weak interfacial adhesion between the matrix and the non-functionalised GNPs.

The incorporation of the GNPs has a negative effect on both the tensile strength and elongation at break, see Fig. 5(b) and (c), respectively. The addition of even modest amounts of GNPs (i.e. 0.5 wt%) leads to a marked decrease in both properties. The tensile strength decreases from 79.0 ± 3.1 MPa for the unmodified epoxy to 50.7 ± 1.3 MPa for the 0.5 wt% GNP/epoxy nanocomposite, and similarly the elongation at break reduces from 4.90 ± 1.24% to 2.47 ± 0.19%. Both properties show a further deterioration, although slight, for higher filler contents, as shown in Fig. 5. This is due to the rigid nature of the GNPs and the relatively poor interfacial adhesion, so the GNPs act as defects resulting in relatively more brittle behaviour of the samples at relatively high loadings.

4.2.4. Electrical conductivity

The electrical conductivity of the GNP-modified epoxy nanocomposites was determined as a function of frequency using electrical impedance spectroscopy (EIS), see Fig. 6(a). The conductivity of the unmodified epoxy is frequency-dependent, which is characteristic of an insulator [24]. The same applies for the 0.5 wt% GNP-containing nanocomposite. Addition of higher filler loadings (i.e. 1.5 wt% and 3 wt%) results in electrically-conductive nanocomposites, since the conductivity is essentially independent of frequency, see Fig. 6(a).

Fig. 6(b) shows the conductivity measured at a frequency of 1 Hz (which is used as the benchmark frequency) versus filler loading. The typical coefficient of variation for the electrical conductivity values determined from the experiments was ±13%. The conductivity increases

Table 1
Thermo-mechanical properties of the GNP-modified epoxy nanocomposites as measured by dynamic mechanical thermal analysis (DMTA).

Filler concentration [wt%]	Storage modulus at 35 °C ($E_g^{'}$) [GPa]	Storage modulus at 180 °C ($E_r^{'}$) [MPa]	Glass transition temperature (T_g) [°C]
0	2.56	2.2	93.2
0.5	2.59	6.7	94.5
1.5	2.65	10.0	94.4
3	2.80	13.6	96.0

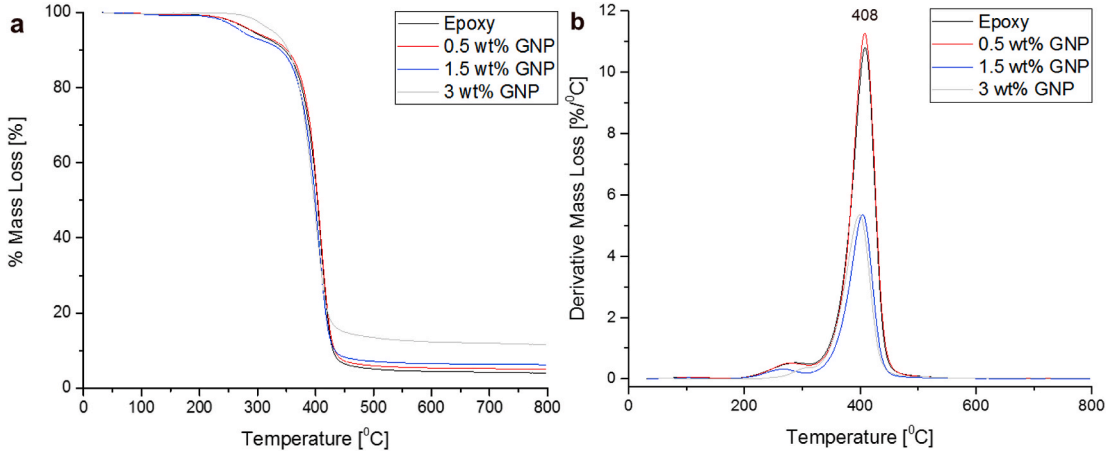

Fig. 4. Thermal stability of the epoxy nanocomposites measured using thermogravimetric analysis (TGA), showing (a) mass loss and (b) derivative mass loss. Samples were heated from 30 to 800 °C at a heating rate of 10 °C/min in a nitrogen atmosphere.

Table 2
Thermogravimetric analysis (TGA) data for the GNP-modified epoxy nanocomposites. Samples were heated from 30 °C to 800 °C at a heating rate of 10 °C/min in a nitrogen atmosphere.

GNP concentration [wt%]	Temperature of 5% mass loss ($T_{5\%}$) [°C]	Temperature of 50% mass loss ($T_{50\%}$) [°C]	Temperature of maximum degradation (T_{max}) [°C]	Char yield at 800 °C (Y_c) [%]
0	292	403	409	4.1
0.5	292	404	408	5.0
1.5	272	399	404	6.2
3	327	397	398	11.6

significantly, by approximately six orders of magnitude, when the filler loading increases from 0.5 wt% to 1.5 wt%. This indicates the formation of a percolating network in this loading range. A percolation threshold (p_c) value of 1 wt% has been reported for GNP-filled epoxy nanocomposites fabricated by three-roll milling (3RM) [25], which is in excellent agreement with the data in the present work.

4.3. Corrosion performance of coatings

The corrosion performance of the GNP-modified epoxy nanocomposites when used as coatings on mild steel substrates was investigated. Panels with a coating thickness of no greater than 60 μm were immersed in a 3.5 wt% NaCl aqueous solution at room temperature (i.e. 25 °C). The progression of rust on the exposed panels was visually evaluated at 24-h intervals. At the completion of the exposure, the adhesion of the coating to the substrate was determined experimentally using the cross-cut test [20].

Two sets of corrosion tests were undertaken. In the first set, coatings with a high GNP content (≥0.5 wt%) and an unmodified epoxy control, were exposed for up to 96 h in the saline solution. In the second set, coatings with a low GNP content (≤0.5 wt%) and an unmodified epoxy control were exposed for up to 120 h.

4.3.1. Epoxy coatings with high content GNP loadings (≥0.5 wt%)

For the first set of corrosion tests, coatings modified with 0.5 wt%, 1.5 wt% and 3 wt% GNP were used, accompanied by the unmodified epoxy control. A set of unexposed panels was subjected to the cross-cut test to examine the effect of the nanofiller on the adhesion of the coating to the steel substrate, and the results are shown in Table 3. The cross-cut test for the unmodified epoxy showed zero damage, indicating that the coating has excellent adhesion to the substrate prior to exposure. This excellent adhesion is expected, as epoxies have very good adhesion to metals and find widespread application as corrosion-protection coatings for metal structures [2]. The addition of the nanofiller does not affect the adhesion of the resulting nanocomposite coatings, see Table 3, and the coatings show excellent adhesion. This is because the GNPs are well embedded in the epoxy matrix resulting in the interphase between the metal and the epoxy remaining unaffected by the presence of the nanofiller. Bagherzadeh et al. [6] similarly reported that the adhesion of epoxy coatings modified with up to 5 wt% of nanoclay did not vary, with all coated samples showing perfect adhesion.

For the exposure tests, panels were prepared and immersed in the 3.5 wt% NaCl aqueous solution. Images of the four exposed panels were taken at 24-h intervals, and these images are shown in Fig. 7. Observation after 48 h showed that the 3 wt% GNP-modified epoxy coating gave the worst appearance of the four coatings, with extensive rusting. Examination of the 0.5 wt% and 1.5 wt% GNP coatings using reflected light revealed extensive blistering, while the unmodified epoxy coating remained largely unaffected by the corrosive environment. After 72 h of exposure the previously-formed blisters for the GNP-modified coatings (i.e. 0.5 wt%, 1.5 wt% and 3 wt%) grew in size and changed colour to become darker brown. For the 0.5 wt% and 3 wt% GNP coatings rust spots were clearly visible across the surface, see Fig. 7. The unmodified epoxy coating remained unaffected by blistering. The appearance of the panels at the end of the exposure period (i.e. 96 h) was not significantly different to that at 72 h, apart from a steady increase in the size of blisters for the GNP-modified coatings. The exposure of the panels was stopped after 96 h, as the 3 wt% panel showed signs of extensive rust.

Following removal from the corrosive environment after 96 h, the panels were conditioned overnight in an oven at 23 °C. The panels were subjected to the cross-cut test to determine the degree of adhesion between the coating and the substrate, and the results are presented in Table 4.

As evaluated using the cross-cut test, the unmodified epoxy coating shows excellent adhesion to the substrate after exposure to the corrosive environment for 96 h, reflecting its visual appearance. The GNP-modified panels demonstrated a relatively large variation across different regions. The reported damage area is the average of the individual values, which are listed as 'damage area values' in Table 4. The damage area percentage was converted to the equivalent classification based on the Standard [20], as outlined in Section 3.5. The general trend identified is that by increasing the amount of nanofiller the corrosion performance of the nanocomposite coatings deteriorates.

Fig. 8 shows images of the 0.5 wt%, 1.5 wt% and 3 wt% GNP panels after the cross-cut tests following exposure to a 3.5 wt% NaCl aqueous solution for 96 h. These images are indicative of the quality of adhesion between the coating and the substrate. Parts of the coating which have been peeled off during the cross-cut tests are visible as the metallic areas

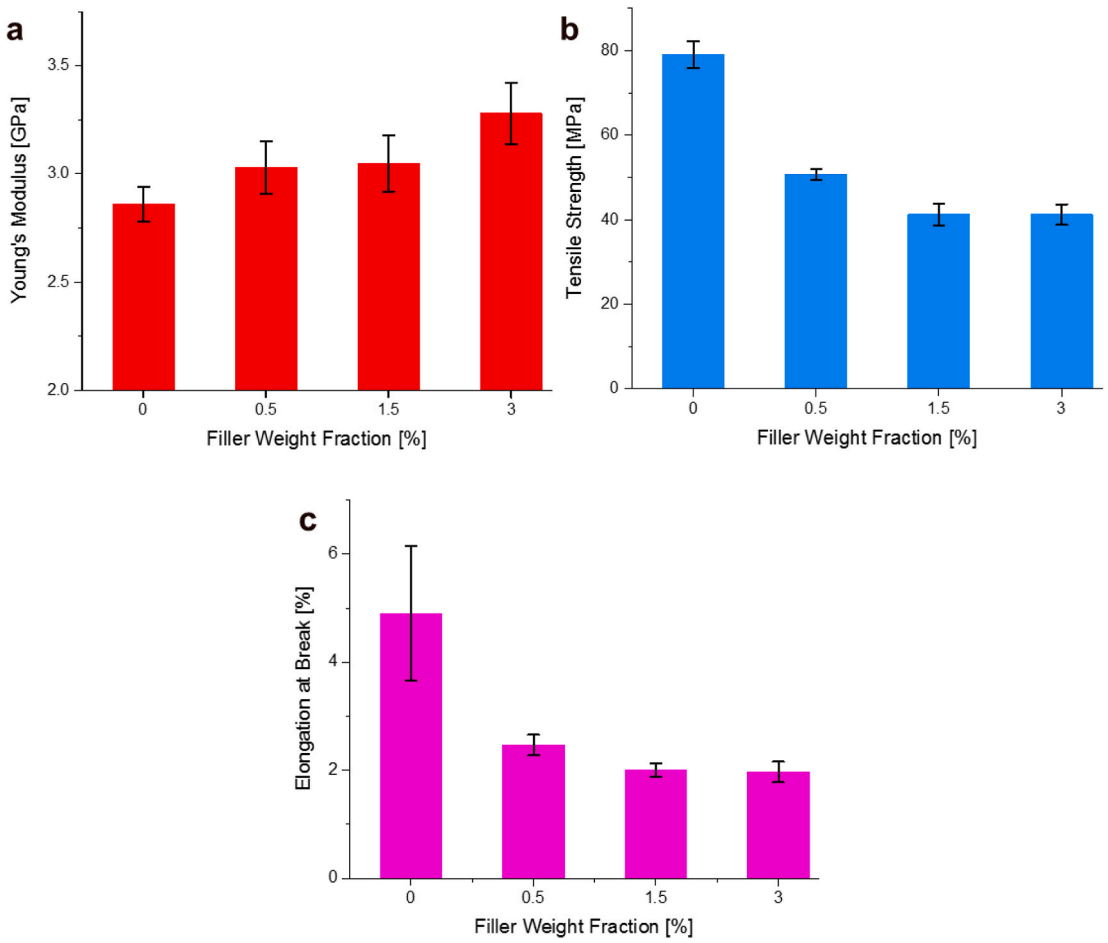

Fig. 5. (a) Young's modulus, (b) tensile strength and (c) elongation at break of the GNP-modified epoxy nanocomposites.

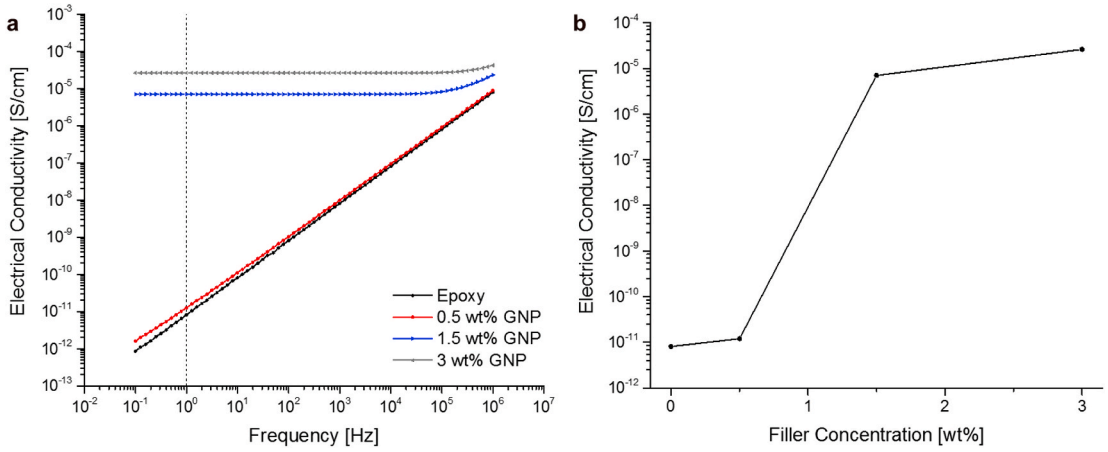

Fig. 6. (a) Log-log plot of the electrical conductivity of the GNP-modified epoxy nanocomposites versus frequency. A frequency of 1 Hz is used for comparison as indicated by the dashed line. (b) Semi-log plot of the electrical conductivity at 1 Hz versus filler loading.

in Fig. 8, as the steel substrate has been exposed. Note that the panels are 15 × 10 cm^2 in dimensions, and the cross-cut test scribes a grid of approximately 2.5 × 1.5 cm^2. For the panel which exhibits the highest degree of damage (i.e. 3 wt% GNP) the detached areas of the coating extend further than the scribed grid, see Fig. 8(c). This qualitative indication of the very poor adhesion confirms the cross-cut test results, see Table 4. The extent of detachment is lower for the 1.5 wt% panel, see Fig. 8(b). For the 0.5 wt% panel, see Fig. 8(a), detachment was only within the scribed area. It can be concluded that panels with a lower GNP content suffered from less damage when subjected to the cross-cut test after exposure.

4.3.2. *Epoxy coatings with low content GNP loadings (≤0.5 wt%)*

From the above observations, it was clear that the incorporation of higher loadings of GNPs deteriorated the performance of the epoxy coatings. Greater amounts of graphene nanofiller might be expected to enhance the corrosion resistance of the coatings, by creating a tortuous path for the diffusion of electrolytes [26]. However, this was not the case

Table 3
Cross-cut test results of unexposed high content GNP-modified epoxy coatings.

Material	Coating thickness [μm]	Cross-cut classification	Damage area [%]	No. of determinations
Epoxy	44 ± 9	0	0%	3
0.5 wt% GNP	48 ± 10	0	0%	3
1.5 wt% GNP	44 ± 4	0	0%	3
3 wt% GNP	20 ± 5	0	0%	3

as seen from the experimental observations and the subsequent cross-cut tests. Hence it was useful to investigate whether coatings with a reduced (≤0.5 wt%) GNP content would perform better than their high content (≥0.5 wt%) counterparts.

Therefore, panels were prepared using between 0 and 0.5 wt% of nanofiller. The GNP-modified epoxy formulations considered were: (a) 0.125 wt%, (b) 0.25 wt%, (c) 0.5 wt% and (d) the unmodified epoxy, as the reference panel. (The 0.5 wt% loading was previously tested but was repeated to enable comparison between the batches).

Unexposed panels of the 0.125 wt% and 0.25 wt% GNP/epoxy coatings were subjected to the cross-cut test to examine the effect of the low content of nanofiller on the adhesion of the coatings to the steel

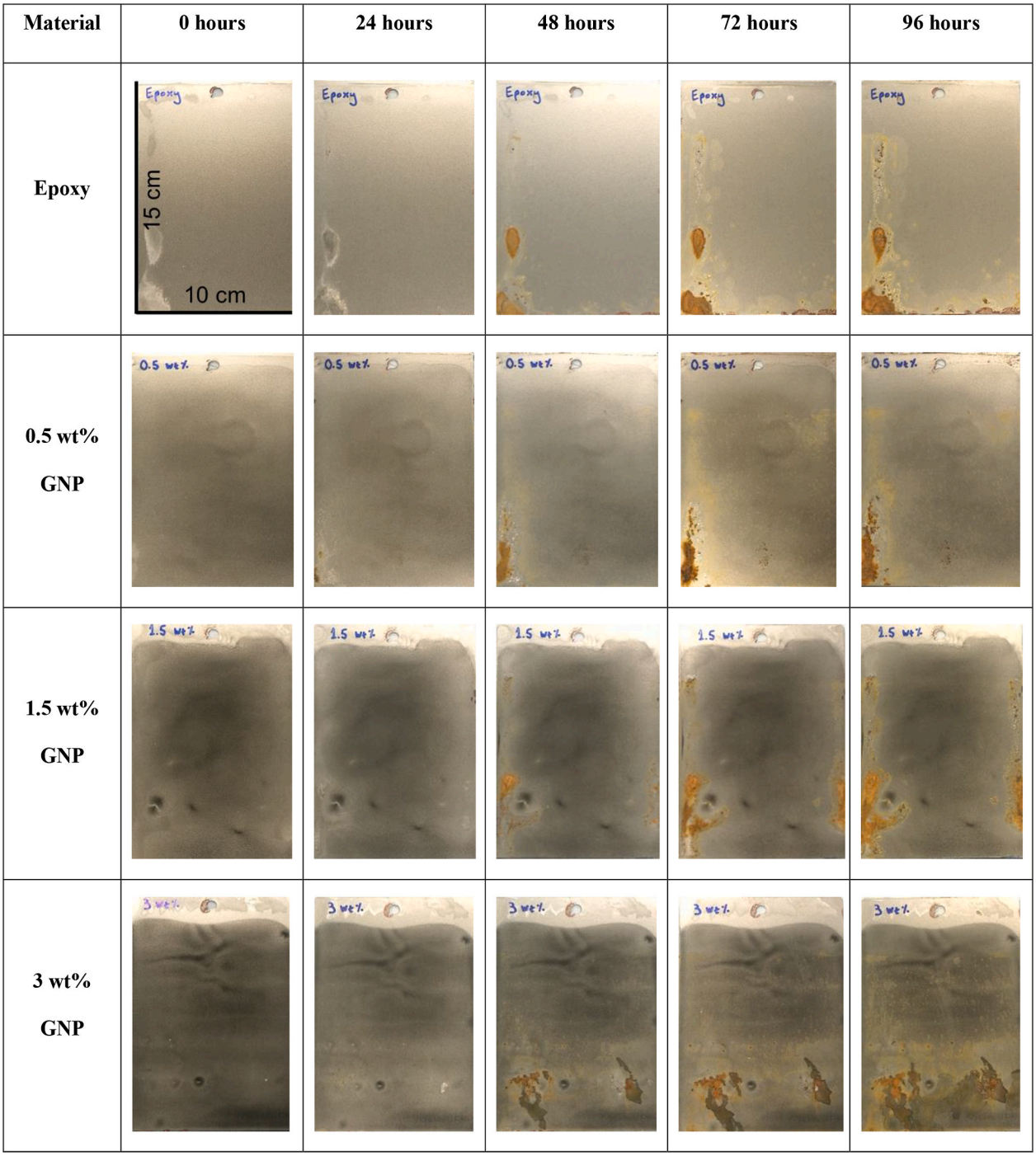

Fig. 7. Test panels of the epoxy coatings, unmodified and modified with a high content of GNPs (at ≥ 0.5 wt%) before (i.e. 0 h) and after exposure in 3.5 wt% NaCl aqueous solution (at 24, 48, 72 and 96 h). The panels measure 15 × 10 cm^2, as indicated at the top left.

Table 4
Cross-cut test results of high content GNP-modified epoxy coatings exposed to a 3.5 wt% NaCl aqueous solution for 96 h.

Material	Coating thickness [μm]	Cross-cut classification	Damage area [%]	Damage area values [%]
Epoxy	36 ± 10	0	0%	0, 0, 0, 0
0.5 wt% GNP	28 ± 10	3	35%	0, 10, 24, 40, 100
1.5 wt% GNP	39 ± 6	4	53%	16, 16, 32, 100, 100
3 wt% GNP	17 ± 4	5	91%	76, 96, 100

substrate, and the results are presented in Table 5. The two panels demonstrate excellent adhesion to the metal, as evidenced by a 0% damage area after the conduct of the cross-cut test. This is consistent with the previous findings reported in Table 3, and is attributed to the excellent adhesion of epoxies to metals which is unaffected by the nanofiller.

Panels of the four formulations was exposed to the 3.5 wt% NaCl aqueous solution for 120 h and photographed at 24-h intervals. Fig. 9 shows images of the four panels at 48, 96 and 120 h of exposure. After complete removal from the corrosive environment at 120 h all of the coatings had developed blisters, which covered an area of between 10 and 50% of the panel surface (with this percentage varying between panels). None of the panels showed significant corrosion, apart from occasional rust spots, see Fig. 9. This is in contrast to the appearance of the more highly filled (i.e. ≥ 0.5 wt% GNP content) coatings after 96 h of exposure, see Fig. 7.

After the conclusion of the exposure test, the panels were conditioned overnight inside an oven at 23 °C and were then subjected to the cross-cut test to determine the degree of adhesion between the coating and the substrate. The adhesion results are presented in Table 6. All four panels showed zero damage following the conduct of the cross-cut test, despite exposure to the 3.5 wt% NaCl aqueous solution for 120 h. This translates to all panels exhibiting excellent adhesion, and the adhesion was consistent across the panel surface. It is notable that for the 0.5 wt% GNP-containing coating a significant variation in the cross-cut damage is observed across the two set of tests. For the panel that was exposed for 120 h zero damage was observed, see Table 6, while for the panel exposed for 96 h a considerably greater degree of damage of 35% was observed, see Table 4. These apparently contradictory results are discussed below when the effect of the GNP content on the corrosion performance of the epoxy coatings is considered.

The above findings clearly demonstrate that epoxy coatings modified with a low content (≤0.5 wt%) of GNPs possess a much-improved anti-corrosion performance compared to high loadings (≥0.5 wt%). The cross-cut tests revealed that low GNP content coatings exhibited perfect adhesion to the steel substrate despite exposure to the corrosive environment for 120 h, see Table 6; while coatings with relatively high GNP contents showed significant damage for an exposure period of just 96 h, see Table 4.

4.4. Effect of GNP content on the corrosion performance of epoxy coatings

The influence of filler material on the corrosion performance of a polymeric coating can be attributed to three considerations; namely, (a) adhesion, (b) alteration to the diffusion path of electrolytes and (c) electrochemical factors. For the unexposed coatings, the presence of the GNP nanofiller did not affect the adhesion of the epoxy to the metal substrate, as the adhesion determined by using the cross-cut test for both the modified and unmodified coatings was excellent. If weak adhesion was present, then the electrolytic species would be able to reach the substrate via the weakly bonded polymer/metal interphase in addition to diffusion through the coating. Consequently, the observed differences in the corrosion performance of the coatings cannot be explained by adhesion considerations.

The barrier properties of GNP/epoxy nanocomposites were studied by Cao [27], who measured the water uptake of bulk epoxy polymers by immersing specimens which were 50 mm in diameter and 3 mm in thickness in deionised water at 50 °C. The experimentally-determined values for the maximum water absorbed at saturation (M_∞) and the diffusion coefficient (D) are shown in Table 7. These results show that GNPs reduce the diffusion coefficient, and that higher contents result in a further suppression of the diffusion rate of water.

Applying Fick's law of diffusion [27,28], it is possible to calculate the

Table 5
Cross-cut test results of unexposed low content GNP-modified epoxy coatings.

Material	Coating thickness [μm]	Cross-cut classification	Damage area [%]	No. of determinations
0.125 wt % GNP	24 ± 5	0	0%	3
0.25 wt% GNP	25 ± 5	0	0%	3

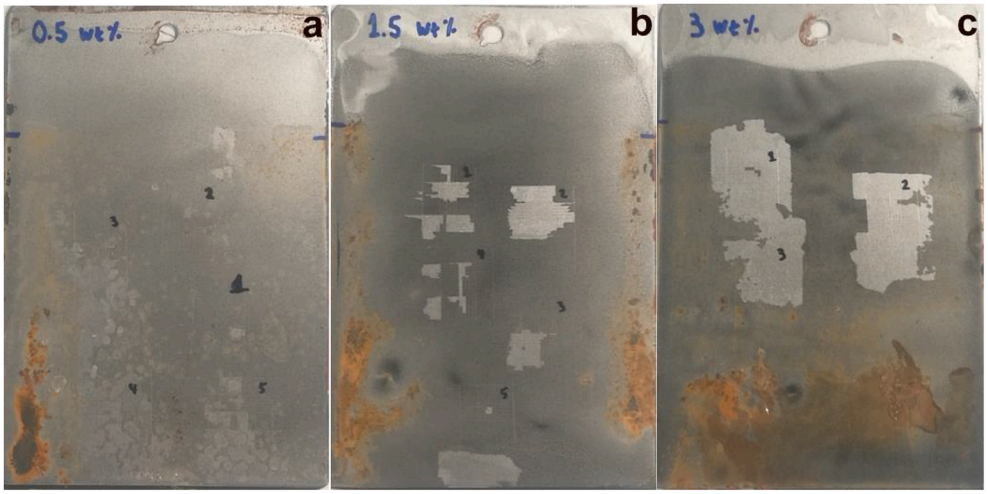

Fig. 8. Images of the exposed (a) 0.5 wt%, (b) 1.5 wt% and (c) 3 wt% high content GNP/epoxy coatings after the conduct of the cross-cut tests after being exposed to a 3.5 wt% NaCl aqueous solution for 96 h.

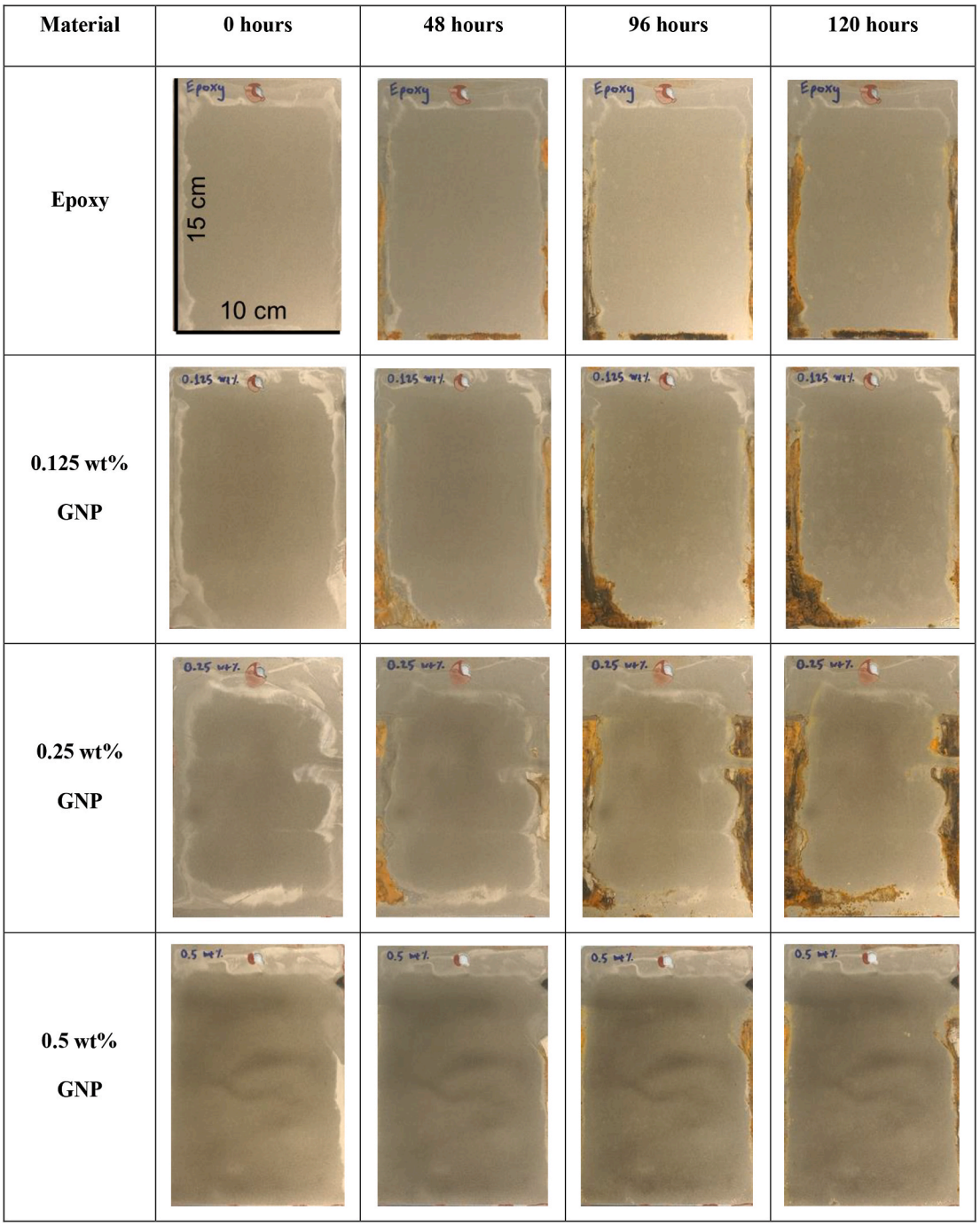

Fig. 9. Panels of the epoxy coatings, unmodified and modified with a low content of GNPs (at ≤ 0.5 wt%) before (0 h) and after exposure in 3.5 wt% NaCl aqueous solution (48, 96 and 120 h). The panels measure 15 × 10 cm^2, as indicated at the top left.

time required for the epoxy coatings to become saturated. Using the smallest reported D value of 3.09×10^{-9} cm^2/s, for the epoxy with 8 wt % of GNPs [27], the maximum saturation time for the coatings can be calculated. In the linear part of diffusion, the weight increase due to water absorption is proportional to the square root of time ($t^{1/2}$) and is described by Equation (1). This equation holds true when the water percentage absorbed is less than 60% of saturation (i.e. $M_t/M_\infty < 0.6$), where M_t is the mass of water absorbed at time t and M_∞ is the mass of water absorbed at saturation [27,28]. The relative water absorption is given by:

$$\frac{M_t}{M_\infty} = \frac{4}{L}\left(\frac{D \times t}{\pi}\right)^{1/2} \quad (1)$$

where L is the coating thickness, D is the diffusion coefficient and t is time.

Assuming that linearity applies up until full saturation (i.e. $M_t/M_\infty = 1$), the time required for full saturation can be calculated by rearranging Equation (1) to give.

$$t = \left(\frac{L}{4}\right)^2 \times \frac{\pi}{D} \quad (2)$$

Table 6
Cross-cut test results of low content GNP-modified epoxy coatings exposed to a 3.5 wt% NaCl aqueous solution for 120 h.

Material	Coating thickness [μm]	Cross-cut classification	Damage area [%]	No. of determinations
Epoxy	33 ± 9	0	0%	5
0.125 wt % GNP	36 ± 7	0	0%	5
0.25 wt% GNP	33 ± 6	0	0%	5
0.5 wt% GNP	37 ± 6	0	0%	6

Table 7
Parameters of water diffusion of GNP/epoxy nanocomposites at 50 °C, as determined experimentally by Cao [27].

GNP loading [wt%]	Water uptake at saturation (M_∞) [wt%]	Diffusion coefficient (D) x 10^{-9} [cm^2/s]
0	2.04 ± 0.01	5.27 ± 0.47
1	2.01 ± 0.03	5.11 ± 0.24
2	2.09 ± 0.02	4.61 ± 0.45
3	2.19 ± 0.02	4.23 ± 0.25
4	2.23 ± 0.03	3.82 ± 0.39
5	2.24 ± 0.07	3.71 ± 0.42
6	2.23 ± 0.09	3.46 ± 0.37
7	2.34 ± 0.06	3.49 ± 0.39
8	2.44 ± 0.01	3.09 ± 0.13

Taking L to be equal to 35 μm (which is a representative thickness of the coatings used in the present work), the epoxy coating becomes fully saturated within 800 s (i.e. approximately 13 min). This indicates that the epoxy coatings (with thicknesses in the range between 20 and 50 μm) became fully saturated within minutes. Therefore, improvements in the D values are not of importance for GNP loadings up to 8 wt%, as an 8 wt% loading only reduced the value of D by about 40% compared to the unmodified epoxy, see Table 7. Consequently, the addition of GNPs is not sufficient to slow down significantly the diffusion of electrolytes through the epoxy matrix, since water manages to reach the steel substrate in minutes. Note that these reported values correspond to the diffusion of water at 50 °C, and that the D values at 25 °C will be approximately three times lower (calculated using the Arrhenius equation), but such a variation is insignificant considering the timescales involved in the immersion tests in the present work.

The speed at which water reaches the metal substrate can be further confirmed by considering the saturated part of diffusion, where water uptake is slower than the linear part described earlier, and which is controlled by the relaxation of water molecules in the polymer matrix [27]. For $M_t/M_\infty > 0.6$, Fick's law is described by [28]:

$$\frac{M_t}{M_\infty} = 1 - \frac{8}{\pi^2} exp\left(\frac{-\pi^2 D t}{L^2}\right) \quad (3)$$

For an immersion time of 1 h (i.e. t = 3600 s), M_t/M_∞ equals 0.99. This confirms that for the D and L values involved in this work, all the coatings become fully saturated within the first hour of immersion in the corrosive environment and that the incorporation of GNPs in the epoxy coating is unable to delay significantly the diffusion of electrolytes to the substrate.

Consequently, the differences in the corrosion behaviour of the panels is due to electrochemical factors. The electrochemical properties of carbon-modified epoxy coatings have been widely reported in the literature and hence the effect of GNPs on the electrochemical corrosion of the epoxy coatings can be deduced. The corrosion potentials (E_{corr}) of selected materials in seawater and temperature of 10 to 27 °C, are presented in Table 8. Materials with a more negative corrosion potential are more active, less noble, forming the anode in an electrochemical cell;

Table 8
Corrosion potentials of materials in seawater at temperature of 10 to 27 °C (reference electrode: saturated calomel electrode (SCE)).

Material	Corrosion potential (E_{corr}) [mV]	Reference
Zinc	−1000	[29]
Mild steel	−700 to − 600	[29]
Graphite epoxy composite	+120	[30]
Graphite	+200 to + 300	[29]

while those with a more positive value are more passive, nobler and form the cathode of an electrochemical cell. The E_{corr} of uncoated bulk epoxy polymers has not been reported in the literature, but the E_{corr} value of a graphite epoxy composite material has been reported (see Table 8). For comparison purposes, the E_{corr} of the graphite epoxy composite material can be considered similar to that of an epoxy polymer. Therefore, coating a steel substrate with an epoxy coating shifts the E_{corr} from −600 mV (for bare steel) to +120 mV, and this increase in the corrosion potential makes the coated steel more passive to corrosion.

The incorporation of GNPs to the epoxy matrix should in theory promote the galvanic corrosion of steel, in an opposite mechanism to that of zinc-rich epoxies. Zinc is a widely-employed filler in the development of anti-corrosive epoxy coatings, due to its sacrificial action [1]. As zinc is more corrosion active than steel, see Table 8, it corrodes preferentially, forming the anode in the galvanic cell and offering cathodic protection to the steel substrate [3]. As GNPs are a graphite-related and highly noble material, they are considerably more passive to corrosion than steel. The GNP nanofiller in the epoxy matrix is therefore expected to lead to the galvanic corrosion of the steel substrate.

The above argument is confirmed from electrochemical studies. Shen et al. [31] reported that the E_{corr} of epoxy coatings decreased with increased contents of multiwalled carbon nanotubes (MWCNTs) for filler loadings ranging between 2 and 8 wt%, reducing from −395 mV for 2 wt % to −432 mV for 8 wt%. Kumar et al. [32], reported a gradual increase in the E_{corr} of MWCNT-filled epoxy coatings for low contents; increasing from −536 mV for the unmodified epoxy to −484 mV for a 0.75 wt% loading. When the filler loading was increased further to 1 wt% there was a decrease in E_{corr} to −580 mV, which was even lower than that of the unmodified epoxy (i.e. −536 mV). The above studies show a clear trend whereby addition of loadings greater than 1 wt% of MWCNTs result in nanocomposite coatings which are more prone to corrosion than the unmodified epoxy, as evidenced by the reduction in the E_{corr} values, and this increase in the corrosion activity is even more pronounced with higher loadings of nanofiller.

Another electrochemical factor is the current of corrosion, I_{corr}. In general, the application of coatings restricts the corrosion of metal substrates by acting as a highly electrically resistive interphase between the substrate and the corrosive environment. This prevents the formation of a complete electrochemical cell [33] as an electrically insulating environment results in low corrosion current. An increase in the I_{corr} with increasing nanocarbon loadings has been confirmed by electrochemical studies. Shen et al. [31] reported that the I_{corr} for MWCNT-filled epoxy coatings increased from 1.5×10^{-9} A/cm^2 for 2 wt % to 9.5×10^{-8} A/cm^2 for 8 wt% MWCNT. Consequently, the intrinsic conductivity of the GNP/epoxy coatings plays a significant role in their poor anti-corrosion performance.

Fig. 6 shows the electrical conductivity of the GNP-modified bulk epoxy polymers. The addition of higher loadings of GNPs (i.e. 1.5 wt% and 3 wt%) results in an increase of approximately six orders of magnitude compared to the unmodified epoxy (which demonstrates a conductivity of 10^{-11} S/cm). On the contrary, the addition of the nanofiller at low loadings (i.e. ≤ 0.5 wt%) did not result in a significant increase; indicating that the nanocomposites with a filler content between 0 wt% and 0.5 wt% demonstrate an electrical conductivity which is almost identical to that of the unmodified epoxy. As shown in Fig. 6

(b), there is a large increase in the electrical conductivity in the region between 0.5 wt% and 1.5 wt%, which coincides with the formation of a percolated network (p_c). This agrees well with the reported p_c value of 1 wt% for GNP/epoxy nanocomposites prepared by three-roll milling (3RM) [25,34].

It is interesting to note that the epoxy coating containing 0.5 wt% GNP demonstrates a non-homogeneous corrosion behaviour, as its filler loading is close to the percolation threshold. As reported earlier the p_c value of some GNP-modified epoxies is at 1 wt% [25,34], while a loading of 0.5 wt% has been shown to be sufficient to form a conductive nanocomposite for a different epoxy system [35]. Taking into consideration the slightly inhomogeneous dispersion of the GNPs in the epoxy matrix (agglomerated regions are clearly seen by a darker colouration in the coating, see Figs. 7 and 9), it is highly likely that localised conductive networks will have formed across areas of the coating allowing conduction from the surface of the coating to the substrate. That means that the corrosion rate will vary across the coated area, being considerably more rapid in areas where the agglomeration is greater and localised networks have formed. This would explain why the 0.5 wt% coating demonstrated variations in its corrosion behaviour across replicate panels, as for the difference in damage shown between panels exposed for 96 h and 120 h, see Tables 4 and 6 respectively.

Based on the findings of Fig. 9, coatings modified with a low content of GNPs (i.e. $\leq$ 0.5 wt%) demonstrate anti-corrosion performance which is comparable to the unmodified epoxy coating. This is expected as the low content coatings will exhibit very comparable E_{corr} values to the unmodified epoxy, and would therefore demonstrate an equally passive behaviour to corrosion. In addition, low content coatings are electrically insulating, thus restricting the conduct of electrochemical reactions across the substrate/coating interphase. No variation in the performance of the low-content coatings and the unmodified epoxy is measured due to the fact that the cross-cut test is not a highly discriminating technique and cannot differentiate clearly between coatings where the variations in concentrations for the 0 to 0.5 wt% range are very small. The superior corrosion behaviour of low-content filled GNP/epoxy coatings agrees very well with the literature. Potentiodynamic polarisation measurements have shown that incorporation of low loadings, of up to 0.5 wt% of graphene, improved the anti-corrosion behaviour compared to unmodified epoxies coated onto metallic substrates [9,11–13]. In these studies, a graphene concentration of 0.5 wt% was reported to result in a simultaneous increase in the E_{corr} and decrease in the I_{corr} values (from interpretation of the Tafel plots). However, no explanation was provided as to why the addition of electrically-conductive graphene leads to a reduction in the I_{corr}.

On the contrary, addition of higher contents of GNPs (i.e. $\geq$ 0.5 wt%) leads to a profound decrease in the E_{corr} values, ultimately making the resulting coatings considerably more prone to corrosion. More detrimental still is the increase in the electrical conductivity of the highly-filled coatings (i.e. 1.5 wt% and 3 wt%) which severely compromises the anti-corrosion performance by allowing the formation of an electrochemical cell between the metal surface, the epoxy coating and the aqueous solution. This explanation is supported from electrochemical data for epoxy coatings modified with high contents of electrically conductive carbon nanofillers [31,32].

5. Conclusions

Graphene due to its unique two-dimensional (2D) geometry, large surface area and impressive impermeability seems to hold promise as filler material for the development of anti-corrosion barrier coatings. In this study, the corrosion resistance of epoxy coatings, unmodified and modified with graphene nanoplatelets (GNPs), coated onto mild steel substrates has been characterised. Coated panels were exposed to an aqueous solution of 3.5 wt% NaCl and the coating adhesion was measured using the cross-cut test.

The incorporation of higher loadings of GNPs ($\geq$0.5 wt%) in an epoxy polymer was seen to decrease the anti-corrosion performance of the resulting coatings. The cross-cut test results for coatings that were exposed to the corrosive medium for 96 h showed that the most highly filled coatings demonstrated the highest degree of damage, with a damage area of 91% and 53% for the 3 wt% and 1.5 wt% modified coatings, respectively; compared to 0% for the unmodified epoxy coating. These results do not agree with the improvement in barrier properties of epoxy polymers reported in the literature via the addition of GNPs. However, by applying Fick's law of diffusion it has been demonstrated that the reductions in the diffusion coefficient are not sufficient to significantly delay the diffusion of water into the coatings. Indeed, electrochemical factors appear to dictate the corrosion behaviour of the coatings with incorporation of higher GNP loadings ($\geq$0.5 wt %) leading to an increase in the corrosion current. This is due to the formation of a percolated network resulting in electrically conductive coatings that facilitate the conduction of corrosion currents. There is a direct correlation between deteriorating corrosion performance and high electrical conductivity, with the worst performing coatings, modified with 3 wt% and 1.5 wt% of GNPs, demonstrating a higher electrical conductivity by six orders of magnitude compared to the unmodified epoxy.

In contrast, the addition of low GNP filler contents ($\leq$0.5 wt%) does not lead to a significant difference in the corrosion behaviour of the nanocomposite coatings in comparison to the unmodified epoxy coating. Epoxy coatings modified with up to 0.5 wt% GNPs demonstrated an identical corrosion performance to the unmodified epoxy, showing zero damage after the adhesion cross-cut test following an exposure period of 120 h. This is suggested to be due to the insulating nature of GNP/epoxy coatings at loadings below the percolation threshold.

Funding

This work was supported by the UK Engineering and Physical Sciences Research Council (EPSRC) [grant number EP/K016792/1]; and the Department of Mechanical Engineering, Imperial College London, UK.

Acknowledgements

Part of this work was funded by the UK Engineering and Physical Sciences Research Council (EPSRC), Grant Number EP/K016792/1. Sotirios Kopsidas would like to acknowledge the Department of Mechanical Engineering, Imperial College London, UK for funding his PhD studentship. The authors would like to thank Dr Phillippe Christou and Dr Nicolas Gogibus of Huntsman Advanced Materials, as well as Dr Stephan Sprenger of Evonik Industries for supplying the epoxy resins and curing agent used in this work.

References

[1] Kouloumbi N, Pantazopoulou P, Moundoulas P. Anticorrosion performance of epoxy coatings on steel surface exposed to deionised water. Pigment Resin Technol 2003;32(2):89–99. https://doi.org/10.1108/03699420310464793.
[2] Ellis B. Chemistry and technology of epoxy resins. Dordrecht, Netherlands: Springer Netherlands; 1993.
[3] Shirehjini FT, Danaee I, Eskandari H, Zarei D. Effect of nano clay on corrosion protection of zinc-rich epoxy coatings on steel 37. J Mater Sci Technol 2016;32 (11):1152–60. https://doi.org/10.1016/j.jmst.2016.08.017.
[4] Li P, He X, Huang T-C, White KL, Zhang X, Liang H, et al. Highly effective anti-corrosion epoxy spray coatings containing self-assembled clay in smectic order. J Mater Chem A 2015;3(6):2669–76. https://doi.org/10.1039/C4TA06221C.
[5] Gorrasi G, Tortora M, Vittoria V, Pollet E, Lepoittevin B, Alexandre M, et al. Vapor barrier properties of polycaprolactone montmorillonite nanocomposite: effect of clay dispersion. Polymer 2003;44(8):2271–9. https://doi.org/10.1016/S0032-3861(03)00108-3.
[6] Bagherzadeh MR, Mahdavi F. Preparation of epoxy–clay nanocomposite and investigation on its anti-corrosive behavior in epoxy coating. Prog Org Coat 2007; 60:117–20. https://doi.org/10.1016/j.porgcoat.2007.07.011.
[7] Papageorgiou DG, Kinloch IA, Young RJ. Mechanical properties of graphene and graphene-based nanocomposites. Prog Mater Sci 2017;90:75–127. https://doi.org/10.1016/j.pmatsci.2017.07.004.

[8] Prasai D, Tuberquia JC, Harl RR, Jennings GK, Rogers BR, Bolotin KI. Graphene: corrosion-inhibiting coating. ACS Nano 2012;6(2):1102–8. https://doi.org/10.1021/nn203507y.
[9] Chen C, Qiu S, Cui M, Qin S, Yan G, Zhao H, et al. Achieving high performance corrosion and wear resistant epoxy coatings via incorporation of noncovalent functionalized graphene. Carbon 2017;114:356–66. https://doi.org/10.1016/j.carbon.2016.12.044.
[10] Mohammadi S, Afshar Taromi F, Shariatpanahi H, Neshati J, Hemmati M. Electrochemical and anticorrosion behavior of functionalized graphite nanoplatelets epoxy coating. J Ind Eng Chem 2014;20(6):4124–39. https://doi.org/10.1016/j.jiec.2014.01.011.
[11] Kumar A, Anant R, Kumar K, Chauhan SS, Kumar S, Kumar R. Anticorrosive and electromagnetic shielding response of a graphene/TiO_2–epoxy nanocomposite with enhanced mechanical properties. RSC Adv 2016;6(114):113405–14. https://doi.org/10.1039/C6RA15273B.
[12] Liu D, Zhao W, Liu S, Cen Q, Xue Q. Comparative tribological and corrosion resistance properties of epoxy composite coatings reinforced with functionalized fullerene C60 and graphene. Surf Coating Technol 2016;286:354–64. https://doi.org/10.1016/j.surfcoat.2015.12.056.
[13] Liu S, Gu L, Zhao H, Chen J, Yu H. Corrosion resistance of graphene-reinforced waterborne epoxy coatings. J Mater Sci Technol 2016;32(5):425–31. https://doi.org/10.1016/j.jmst.2015.12.017.
[14] Chang K-C, Hsu M-H, Lu H-I, Lai M-C, Liu P-J, Hsu C-H, et al. Room-temperature cured hydrophobic epoxy/graphene composites as corrosion inhibitor for cold-rolled steel. Carbon 2014;66:144–53. https://doi.org/10.1016/j.carbon.2013.08.052.
[15] Graphene Supermarket. Graphene nanopowder: 12 nm flakes-25 g. Available from: https://graphene-supermarket.com/Graphene-Nanopowder-AO-3-12-nm-Flakes-25-g.html; 25th April 2018.
[16] Q-Lab Corporation. Q-panel steel and iron phosphated panels. Specification bulletin LP-0862-A. Westlake, USA: Q-Lab Corporation; 2015.
[17] Plastics - determination of tensile properties. Part 1: general principles ISO 527-1: 2012. Geneva, Switzerland: ISO; 2012.
[18] Standard practice for testing water resistance of coatings using water immersion ASTM 870-15. West Conshohocken, USA: ASTM International; 2015. doi:10.1520/D0870-15.
[19] Martí M, Armelin E, Iribarren JI, Alemán C. Soluble polythiophenes as anticorrosive additives for marine epoxy paints. Mater Corros 2015;66(1):23–30. https://doi.org/10.1002/maco.201307132.
[20] Paints and varnishes - cross-cut test ISO 2409:2013. Geneva, Switzerland: ISO; 2013.
[21] Chandrasekaran S, Seidel C, Schulte K. Preparation and characterization of graphite nano-platelet (GNP)/epoxy nano-composite: mechanical, electrical and thermal properties. Eur Polym J 2013;49(12):3878–88. https://doi.org/10.1016/j.eurpolymj.2013.10.008.
[22] Olowojoba GB, Kopsidas S, Eslava S, Gutierrez ES, Kinloch AJ, Mattevi C, et al. A facile way to produce epoxy nanocomposites having excellent thermal conductivity with low contents of reduced graphene oxide. J Mater Sci 2017;52(12):7323–44. https://doi.org/10.1007/s10853-017-0969-x.
[23] Sang B, Li Z-W, Li X-H, Yu L-G, Zhang Z-J. Graphene-based flame retardants: a review. J Mater Sci 2016;51(18):8271–95. https://doi.org/10.1007/s10853-016-0124-0.
[24] Wang D, Zhang X, Zha J-W, Zhao J, Dang Z-M, Hu G-H. Dielectric properties of reduced graphene oxide/polypropylene nanocomposites with ultralow percolation threshold. Polymer 2013;54:1916–22. https://doi.org/10.1016/j.polymer.2013.02.012.
[25] Li Y, Zhang H, Porwal H, Huang Z, Bilotti E, Peijs T. Mechanical, electrical and thermal properties of in-situ exfoliated graphene/epoxy nanocomposites. Nanocomposites Part A: Appl Sci Manufact 2017;95:229–36.
[26] Rajabi M, Rashed GR, Zaarei D. Assessment of graphene oxide/epoxy nanocomposite as corrosion resistance coating on carbon steel. Corrosion Eng Sci Technol 2015;50(7):509–16. https://doi.org/10.1179/1743278214Y.0000000232.
[27] Cao G. Multifunctional epoxy/graphene nanoplatelet nanocomposites. PhD Thesis. Manchester, UK: University of Manchester; 2016.
[28] Suloff EC. Sorption behavior of an aliphatic series of aldehydes in the presence of poly(ethylene terephthalate) blends containing aldehyde scavenging agents.. PhD Thesis. Blacksburg, Virginia, USA: Virginia Polytechnic Institute and State University; 2002.
[29] Deshpande KB. Validated numerical modelling of galvanic corrosion for couples: magnesium alloy (AE44)–mild steel and AE44–aluminium alloy (AA6063) in brine solution. Corrosion Sci 2010;52(10):3514–22. https://doi.org/10.1016/j.corsci.2010.06.031.
[30] Miller Jr BA. The galvanic corrosion of graphite epoxy composite materials coupled with alloys.. Master of Science Thesis. Wright-Patterson Air Force Base, USA: Air Force Institute of Technology; 1975.
[31] Shen W, Feng L, Liu X, Luo H, Liu Z, Tong P, et al. Multiwall carbon nanotubes-reinforced epoxy hybrid coatings with high electrical conductivity and corrosion resistance prepared via electrostatic spraying. Prog Org Coat 2016;90:139–46. https://doi.org/10.1016/j.porgcoat.2015.10.006.
[32] Kumar A, Ghosh PK, Yadav KL, Kumar K. Thermo-mechanical and anti-corrosive properties of MWCNT/epoxy nanocomposite fabricated by innovative dispersion technique. Nanocomposites Part B 2017;113:291–9. https://doi.org/10.1016/j.nanocompositesb.2017.01.046.
[33] Schriver M, Regan W, Gannett WJ, Zaniewski AM, Crommie MF, Zettl A. Graphene as a long-term metal oxidation barrier: worse than nothing. ACS Nano 2013;7(7):5763–8. https://doi.org/10.1021/nn4014356.
[34] Wu S, Ladani RB, Zhang J, Bafekrpour E, Ghorbani K, Mouritz AP, et al. Aligning multilayer graphene flakes with an external electric field to improve multifunctional properties of epoxy nanocomposites. Carbon 2015;94:607–18. https://doi.org/10.1016/j.carbon.2015.07.026.
[35] Kopsidas S. Multifunctional epoxy nanocomposites modified with graphene nanoplatelets and carbon nanotubes.. PhD Thesis. London, UK: Imperial College London; 2019.